

THE EFFECT OF SOFOSBUVIR ADMINISTRATION ON ALBINO RATS' BUCCAL MUCOSA (HISTOLOGICAL AND IMMUNOCHEMICAL STUDY)

Nakaa Ahmed Mohamed Elbattrick*^{ID}, Ahmed Mahmoud Halawa**^{ID},
Nehad Samir***^{ID} and Safaa Ismail Hussein****^{ID}

ABSTRACT

Introduction: Hepatitis C virus (HCV) infection is a principal cause of mortality globally. About 170 million people were infected with HCV worldwide. Egypt's Ministry of Health and Population has released a nationwide strategy to address this pandemic. Sofosbuvir is a new combination of direct-acting antiviral drugs that doesn't require addition of interferon and is an effective alternative to interferon. The systemic effects of Sofosbuvir are being investigated nowadays; however, there aren't enough studies on its impact on oral health yet.

Aim of the study: To investigate the effect of Sofosbuvir on buccal mucosa in Albino rats.

Materials and Methods: Twenty-eight Adult male albino rats were randomly divided into two main groups, fourteen rats each. Each group was furtherly subdivided into two subgroups A & B according to the time of sacrifice which was 45 and 60 days respectively. *Control group (Group I)* was given distilled water daily by gastric tube, and *experimental group (Group II)* was given Sofosbuvir (40 mg/kg/day) dissolved in distilled water by gastric tube. Specimens were examined histologically and immunohistochemically.

Results: *Group II* showed vacuolization in the epithelium and signs of degeneration in both epithelium and connective tissue. Immunohistochemical results of *Group I* showed strong positive nuclear immunoreactivity for Ki-67 in the epithelial cells and lamina propria, however *Group II* showed weak nuclear immunoreactivity for Ki-67. Statistical results showed significant decrease in Ki-67 positive area percentage of Subgroup IIB when compared to Subgroup IIA.

Conclusion: Sofosbuvir administration resulted in degenerative changes in buccal mucosa and affected its proliferation, which was time dependent.

KEYWORDS: Sofosbuvir; Buccal mucosa; Ki-67 Antibody.

* Demonstrator of Oral Histopathology Faculty of Dentistry, Misr International University, Cairo, Egypt.

** Professor at department of Oral Biology, Faculty of Dentistry, Ain Shams University, Cairo, Egypt.

*** Professor at department of Oral Histopathology, Faculty of Dentistry, Misr International University, Cairo, Egypt.

**** Lecturer at department of Oral Biology, Faculty of Dentistry, Ain Shams University, Cairo, Egypt.

INTRODUCTION

Hepatitis C virus (HCV) is the main etiology of chronic hepatitis and liver lethal diseases. An estimated 170 million people were infected worldwide, with 350,000 people dying each year as a result of this fatal virus ^[1]. The HCV has the ability to cause a chronic infection in about 70% of the cases that lead to the development of many serious liver diseases such as liver cirrhosis and hepatocellular carcinoma. Chronic HCV has a high rank in worldwide morbidity and global suffering ^[2].

The treatment of HCV has undergone a number of advances in recent years, many of which have significantly changed the prognosis. Hence the use of new combination of direct-acting antiviral drugs (DAADs) without interferon (IFN) seems to be a promising treatment alternative therapy method (e.g., Sofosbuvir) ^[3,4].

Sofosbuvir (SOF) is basically a HCV polymerase inhibitor and its chemical formula is C₂₂H₂₉F₃N₃O₉P ^[5]. Sofosbuvir is immediately converted to its active metabolite by enzymes found in the human hepatic cells in the liver. The active nucleotide form is metabolized to the inactive metabolite of the nucleotide, which is mainly removed by passive filtration in the renal glomerulus, and it imitates the physiological nucleotide. It competitively blocks the viral RNA polymerase (NS5B polymerase), thus inhibiting the HCV-RNA formation by RNA chain termination ^[6,7].

This drug is very potent as it has a fortification to resistance and it has a high tolerance response. The dosage is not complicated if compared to other drugs as it is prescribed only once daily by oral administration of a 400mg tablet, this drug is relatively free from major drug-drug interaction ^[8].

The systemic effects of SOF are increasingly investigated nowadays; however, there are no sufficient researches on its effect on the oral health. Furthermore, due to its breakthrough

results in the treatment of HCV internationally, and its easy availability in Egypt, the aim of this study is to investigate the effects of SOF on buccal mucosa of Albino rat histologically and immunohistochemically.

MATERIALS AND METHODS

Materials

Sofosbuvir was obtained in the form of tablets from the local pharmaceutical market under the market name Sovaldi™ by Gilead Sciences pharmaceutical company.

Methodology

A) Animals: Twenty-eight adult male Wistar Albino rats, weight ranging from 200-250 gm were used in this study. Albino rats were collected from the animal house of Ain Shams University. The rats were caged in stainless steel cages with five rats per cage at the Medical Research Center, Ain Shams University. The rats were fed a regular diet of fresh vegetables and bread; they received tap water. The correct ventilation and nutrition conditions that ensure good and clean working environment were followed under the supervision of a specialized veterinarian. The Research Ethics Committee of the Faculty of Dentistry at Ain Shams University reviewed and accepted the protocol, and the final approval number is FDASU-RecIM121801.

B) Animal Grouping: Rats were randomly divided evenly into two main groups, fourteen rats each, as follows in Table (1).

C) Drug Administration: Tablets were crushed and dissolved in distilled water (8mg/ml), then administrated to the albino rats via a gastric tube. The dose used was (40mg/kg/day) ^[9].

At the end of the experiment all animals were euthanized by overdose of anesthesia and immediately dissected to obtain the buccal mucosa. All specimens were processed and prepared to be

TABLE (1): Showing different groups, dose, route of drug administration and sacrifice date.

Grouping	No. of albino rats	Sacrifice date and albino rats no.	
<i>Group I (control)</i>	14	Day 45	<i>Subgroup IA</i> 7 albino rats.
		Day 60	<i>Subgroup IB</i> 7 albino rats.
<i>Group II (experimental) (Sovaldi treated group)</i>	14	Day 45	<i>Subgroup IIA</i> 7 albino rats.
		Day 60	<i>Subgroup IIB</i> 7 albino rats.

stained for histological and immunohistochemical examination using the following stains respectively:

- Hematoxylin & Eosin stain for routine histological examination^[10].
- Immunohistochemically staining using monoclonal Ki-67 antibody.

Ki-67 protein was prepared in mice^[11]. Ki-67 is characterized by nuclear localization. The immunopositive cells are dark brown while the rest are blue^[12].

Methodology of Ki-67 staining:

- Deparaffinization was achieved with xylene then rehydration in graded alcohol solutions.
- The epitopes were extracted by raising the temperature of the sections to 121°C for 10 minutes in citrate buffer (pH6.0).
- To block endogenous activity sections were incubated in 3% hydrogen peroxide (H₂O₂) in methanol for 5 min then blocking of nonspecific binding of primary antibodies to epitopes by a pre-incubation step with 5% regular goat serum for 10 min at 37°C.
- The primary antibody Ki-67 (Dako, M7240, 1:100) was applied on the slides and incubated in humid chamber overnight in refrigerator at 40°C.
- Color development was done with diaminobenzidine (DAB).

The slides were counterstained with haematoxylin, dehydrated in ascending grades of alcohol, cleared in xylene and mounted^[13,14].

Examination and photographing were done for H&E and Ki-67 stained sections using Leica Qwin 500 image analyzer computer system (England). The image analyzer is mainly composed of a colored video camera, colored monitor and a hard disc of IBM personal computer connected to the microscope. This was done at the Research Center of Oral Histopathology Department, Faculty of Dentistry, Misr International University.

Histomorphometric analysis was performed for measuring ki-67 immunostaining. Ki-67 stained sections were randomly selected and the positive area percentage was calculated from five adjacent microscopic fields using image J for analysis, the images were conducted of all specimens at standard magnification × 200.

Statistical analysis:

Numerical data were tested for normality using Shapiro-Wilk test. Data showed parametric distribution so they were presented as mean and standard deviation values and were analyzed using independent t-test for inter and intra group comparison. The significance level was set at $p \leq 0.05$ within all tests. Statistical analysis was performed with R statistical analysis software version 4.1.2 for Windows.

RESULTS

H&E results

Group I (control group): Subgroups IA & IB:

Histological results of the control group showed normal histological features of the buccal mucosa with apparent normal epithelial thickness. The epithelium and the lamina propria were separated by well-defined basement membrane. The epithelial rete pegs appeared short, broad and numerous. The epithelium was underlined with normal fibrous dense connective tissue lamina propria continuous with submucosa and the underlying muscle fibers. The lamina propria consisted of dense vascular connective tissue with fibroblasts and collagen fiber bundles. Submucosa showed collagen fibers and muscle cells **Fig. (1A)**.

Higher magnification of the covering epithelium showed ortho-keratinized stratified squamous epithelium, with normal sized tightly packed epithelial cells with no intercellular bridge disruption and normal nuclei appearance. The basal cells appeared with largely deeply stained nuclei and basophilic cytoplasm. Parabasal cells

appeared polyhedral with rounded nuclei and basophilic cytoplasm. The flat cells of the granular cell layer showed flat deeply stained nuclei and basophilic granules in the cytoplasm. The keratin layer appeared as a well-defined acidophilic layer covering the epithelium **Fig. (1B)**.

Group II

Subgroup IIA: where rats were treated by Sovaldi for 45 days.

By examining the histological sections of (subgroup IIA), the covering epithelium appeared with decreased thickness. The basement membrane appeared irregular with multiple short epithelial rete pegs with irregular thickness. The connective tissue lamina propria of this group appeared as irregularly arranged fibrous layer with areas of separation and dilated blood vessels. The submucosa showed areas of separations especially surrounding the muscle layer **Fig. (2A)**.

Higher magnification of the covering epithelium showed parabasal cell layer appeared with paler cytoplasm, pale stained nuclei and diffuse cytoplasmic vacuolization. Some cells of the spinous

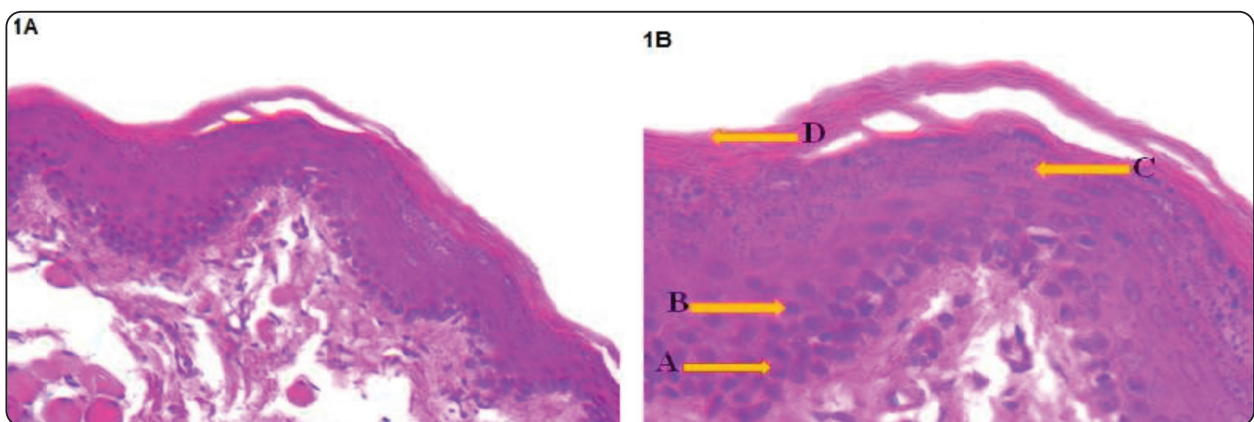


Fig. (1): 1A: Photomicrograph of group I showing buccal mucosa with orthokeratinized stratified squamous epithelium, the epithelial rete pegs are short, broad and numerous. Lamina propria is dense and fibrous. The submucosa shows normal structure. (HX. & E. stain, Orig. Mag., x200), 1B: Higher magnification showing covering epithelium, its basal cell layer cells have deeply stained nucleus and basophilic cytoplasm (A), large polyhedral parabasal cells with rounded nuclei and basophilic cytoplasm (B), granular cell layer with flat deeply stained nuclei and basophilic granules (C), The keratin layer appears as a well-defined layer with eosinophilic stain (D) (HX. & E. stain, Orig. Mag., x400).

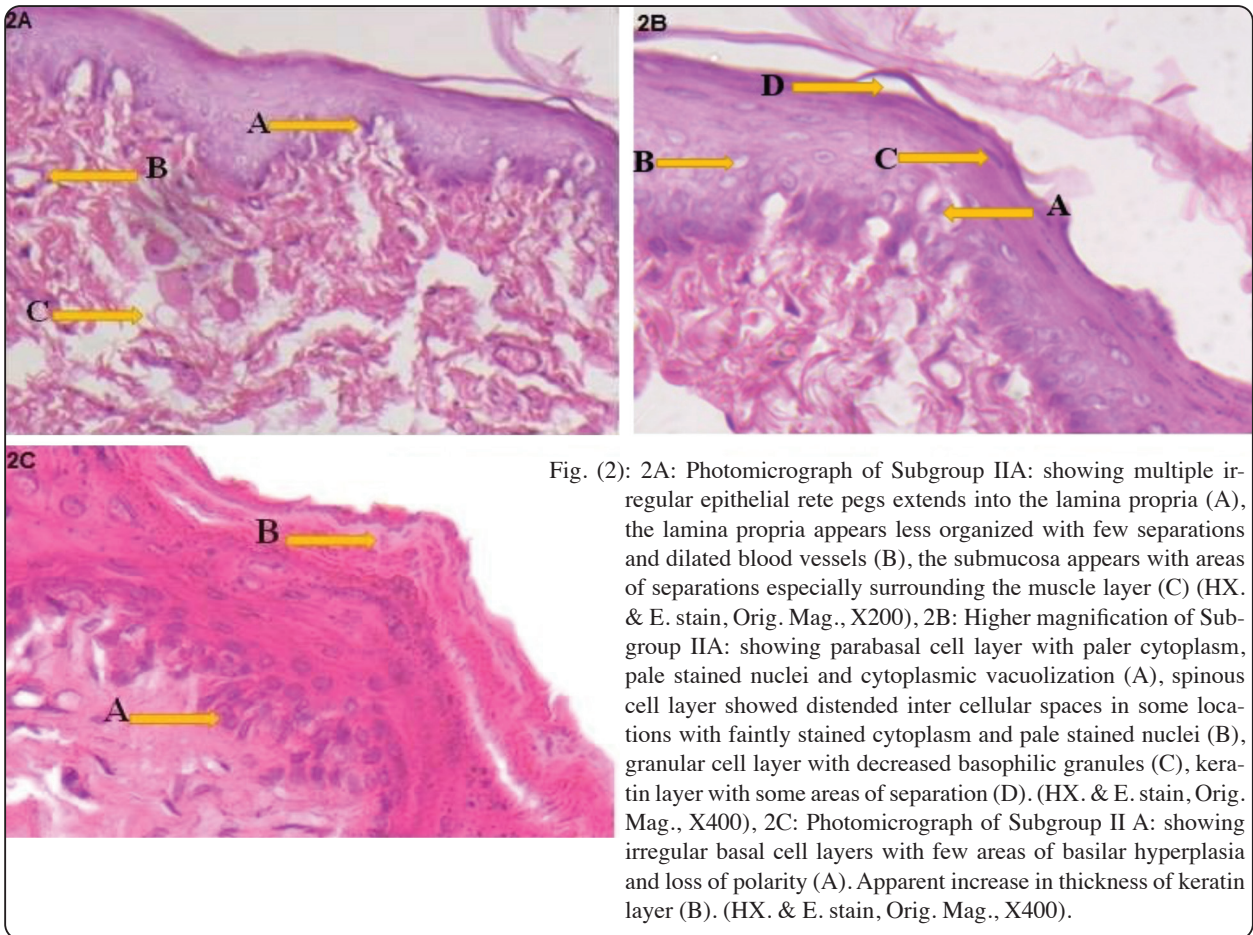


Fig. (2): 2A: Photomicrograph of Subgroup IIA: showing multiple irregular epithelial rete pegs extends into the lamina propria (A), the lamina propria appears less organized with few separations and dilated blood vessels (B), the submucosa appears with areas of separations especially surrounding the muscle layer (C) (HX. & E. stain, Orig. Mag., X200), 2B: Higher magnification of Subgroup IIA: showing parabasal cell layer with paler cytoplasm, pale stained nuclei and cytoplasmic vacuolization (A), spinous cell layer showed distended inter cellular spaces in some locations with faintly stained cytoplasm and pale stained nuclei (B), granular cell layer with decreased basophilic granules (C), keratin layer with some areas of separation (D). (HX. & E. stain, Orig. Mag., X400), 2C: Photomicrograph of Subgroup II A: showing irregular basal cell layers with few areas of basilar hyperplasia and loss of polarity (A). Apparent increase in thickness of keratin layer (B). (HX. & E. stain, Orig. Mag., X400).

cell layer showed distended inter cellular spaces in some locations with faintly stained cytoplasm and pale stained nuclei. The granular cell layer showed decrease in the basophilic granules. The stratum corneum showed some areas of separation within its thickness, some areas show separation from the epithelium **Fig. (2B)**.

In some specimens, a few areas of basilar hyperplasia with loss of polarity and detectable increase in the thickness of keratin layer without separations was seen **Fig. (2C)**.

Subgroup IIB: where rats were treated by Sovaldi for 60 days.

The buccal mucosa was covered by keratinized stratified squamous epithelium. The basement membrane appeared smooth with decreased

scalloping. The papillary layer of the lamina propria appeared to have disorganized connective tissue fiber bundles and the submucosa appeared disorganized with some areas of degeneration and dilated blood vessels **Fig. (3A)**.

On higher magnification, the basal cell layer was composed of a single row of non-columnar cells, some basal and parabasal cells showed signs of degeneration appeared as wide perinuclear haloing and vacuolations. The nuclei of the stratum spinosum appeared obviously pale stained. Some nuclei showed almost complete degeneration in prickle and granular cell layers **Fig. (3B)**.

The thickness of the granular cell layer was markedly diminished and consequently, the amount of keratohyalin granules was fewer. The cornified layer appeared thinner, compared to subgroup IIA

and in some specimens, the keratin layer appeared separated from the underlying epithelium with corrugated surface **Fig. (3B)**. Some regions showed swelling in prickle cells with binucleation and mitotic figures **Fig. (3C)**.

Immunohistochemical results:

GROUP I: (control group)

Subgroup IA: scarified on day 45 SubgroupIB: scarified on day 60.

In both subgroups a strong nuclear immunoreactivity to Ki-67 in the basal, parabasal

cell layer is detected while mild staining reaction is demonstrated in some granular layer cells and the underlying connective tissue. Negative nuclear reaction is rarely observed **Fig. (4A & 4B)**.

GROUP II: (experimental group)

Subgroup IIA: where rats were treated for 45 days (short-term Sovaldi administration).

Immunohistochemical examination of Ki-67 expression in the specimens showed mild nuclear immunoreactivity in basal and parabasal layers, weak staining was observed in granular cell layer and the underlying connective tissue, in addition to

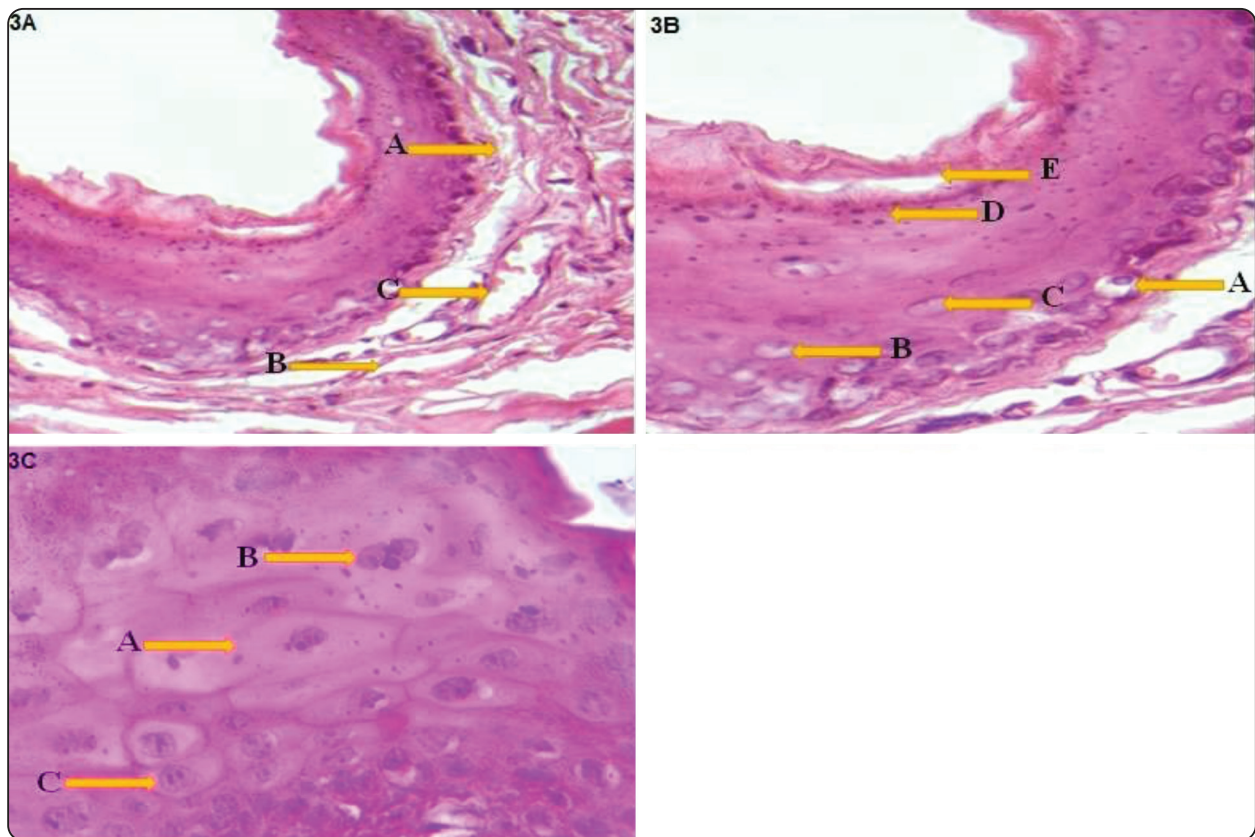


Fig. (3): 3A: Photomicrograph of Subgroup IIB: showing smooth basement membrane. The papillary layer with disorganized connective tissue fiber bundles (A) areas of separations in the submucosa with areas of degeneration (B), dilated blood vessels are seen (C). (HX. & E. stain, Orig. Mag., X200). 3B: Higher magnification showing signs of degeneration in some of the basal and parabasal cells with perinuclear haloing and vacuolations (A), The nuclei of the spinous cell layer are pale stained (B), some nuclei show complete degeneration (C), decreased thickness of the granular cell layer and the amount of keratohyalin granules (D), the keratin layer separated from the underlying epithelium with corrugated surface (E). (HX. & E. stain, Orig. Mag., X400). 3C: Showing swelling in the prickle cell layer (A) with binucleation (B) and mitotic figures (C) (HX. & E. stain, Orig. Mag., X400).

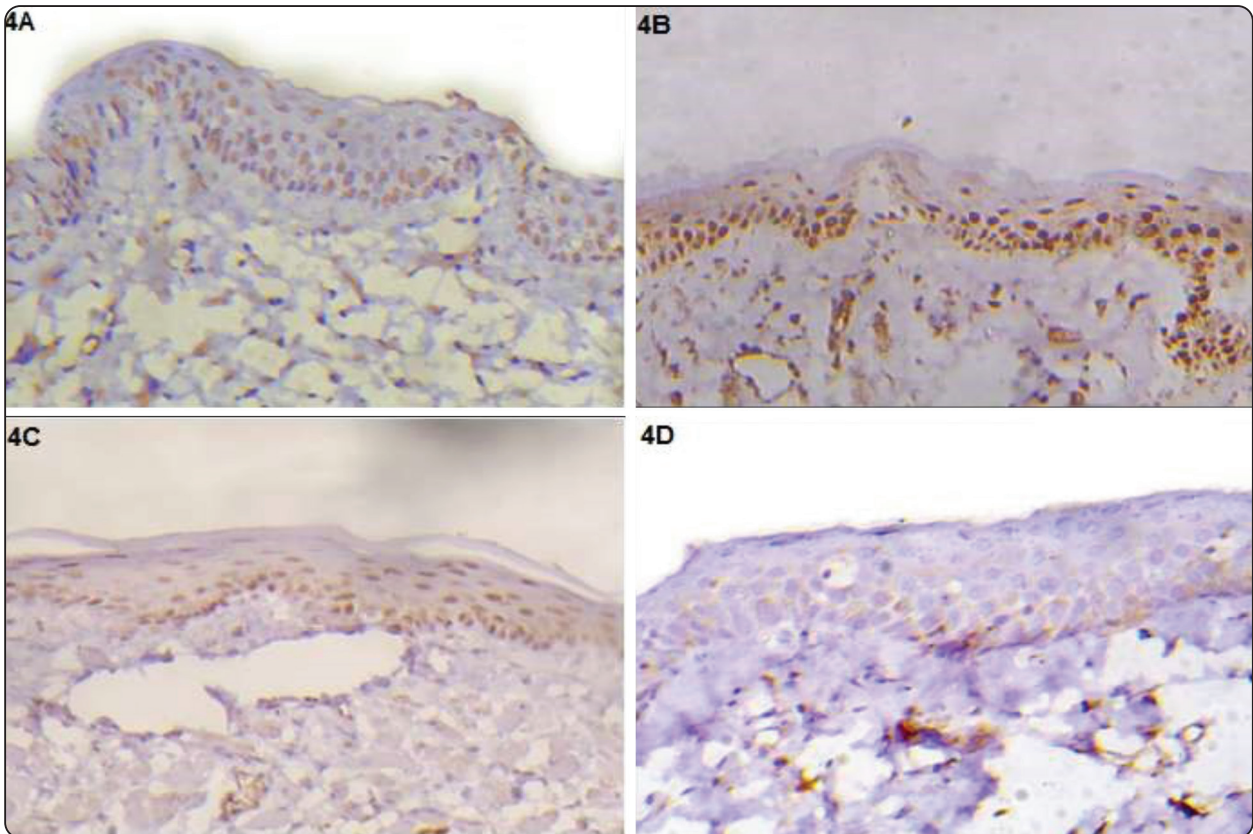


Fig. (4): 4A: Photomicrograph of Subgroup IA: showing strong staining for Ki-67 at basal and parabasal cells, mild staining reaction at the granular cell layer and the connective tissue. 4B: Subgroup IB: showing strong staining for Ki-67 at basal and parabasal cells. Mild staining reaction at the granular cell layer and the connective tissue. 4C: Subgroup IIA: showing mild staining for Ki-67 in the basal and parabasal layer, weak staining at the granular cell layer and the connective tissue. 4D: Subgroup IIB: showing weak staining for Ki-67 at basal, parabasal layer, granular cell layer and connective tissue. (Ki-67, Orig. Mag., X200).

the increase of the negative nuclei. This expression was apparently lower than that detected in group I. **Fig. (4C).**

Subgroup IIB: where rats were treated for 60 days (long-term Sovaldi administration).

Sections presented weak nuclear expression to Ki-67 at basal, parabasal, granular cell layer and the underlying connective tissue; this reactivity to Ki-67 was decreased compared to group I and subgroup IIA with some negative nuclei. **Fig. (4D).**

Statistical results

1-Intergroup comparisons

Using t-test to compare between control and

experimental groups, the mean of area percentage of immunopositive cells, was significantly higher in subgroup IA (87.57 ± 10.15) than subgroup IIA (49.14 ± 5.52) and in subgroup IB (88.57 ± 11.87) than subgroup IIB (33.29 ± 8.71) ($p < 0.001$).

2-Intragroup comparisons

Using t-test to compare between the two different durations of the control group, and compare between the two different durations in the experimental group as well, the mean of area percentage of immunopositive cells, was higher in subgroup IA (87.57 ± 10.15) than subgroup IB (88.57 ± 11.87) yet the difference was not statistically significant ($p = 0.868$). Mean area percentage was significantly

higher in subgroup IIA (49.14±5.52) than subgroup IIB (33.29±8.71) (p=0.002).

Mean and Standard deviation (SD) values for area percentage of cells immunostained with Ki-67 for different subgroups were presented in **table (2)** and **Fig. (5)**.

TABLE (2): Mean and Standard deviation (SD) values for area percentage of immunostained positive cells with Ki-67 for different subgroups.

Time	Area percentage of immunostained positive cells with Ki-67 (Mean±SD)		p-value
	Control (I)	Experimental (II)	
	Day 45	87.57±10.15	
Day 60	88.57±11.87	33.29±8.71	<0.001*
p-value	0.868	0.002*	

*; significant (p ≤ 0.05)

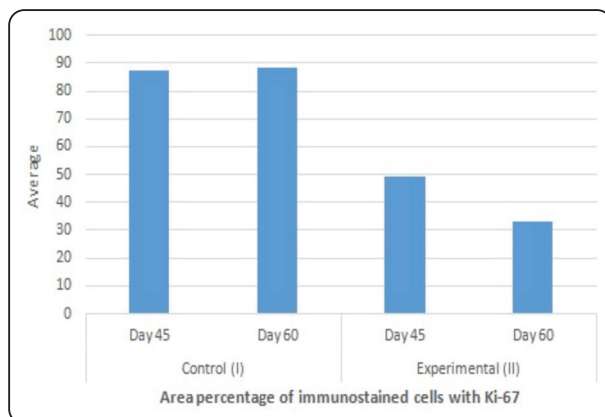


Fig. (5): Bar chart showing average area percentage of cells immunostained with Ki-67 for different subgroups.

DISCUSSION

The main cause of chronic hepatitis and liver lethal diseases is the HCV, patients with HCV are being treated more successfully with the new second-generation of DAADs which include Simeprevir and SOF, which not only increase the effectiveness of the regimens but also the safety profile of it. In Egypt, 25% of the population has been infected with HCV. Accordingly, the Egyptian Ministry of Health and Population proposed a national strategy to control the epidemic HCV, the strategy was by launching the national campaign program “The Plan of Action for the Prevention, Care and Treatment of Viral Hepatitis 2014–2018” which advocated SOF (Sovaldi™) as the primary treatment choice [15,16,17].

In the biomedical research, the laboratory rats are inevitable. They are known as the leading model in many fields and in variety of sectors including viral vaccination, cancer and toxicology studies. The human being is no longer used as an experimental subject. Amongst rodents, rats are mostly used for experimental studies especially for in-vivo studies [18].

The current study evaluated the histological changes in two different durations, forty-five and sixty days of SOF administration. Literature review recommends and the drug pamphlet of Sovaldi™ recommended dose is one of these two durations; which are the most commonly used in therapy regimen [19]. The dose (40 mg/kg/day) was given to the experimental group according to an equation made by [9].

The buccal mucosa was chosen because of its intimate anatomic relationship between the buccinators, and buccal space allowing any potential sign of an abnormal lesion to progress without being obstructed by any anatomical barriers. Furthermore, the buccal mucosa is an easily accessible tissue for sampling [20, 21, 22].

In the current study, the H and E stained sections of SOF- treated rat's buccal mucosa in both subgroups IIA and IIB revealed marked degeneration of the epithelial cells. These findings are consistent with ^[23], who was studying the effect of SOF on the rats' kidneys, they found degenerated epithelial cells and with different degrees of degeneration in the nuclei (karyorrhexis, karyolysis or loss).

In the current study, Subgroup IIA showed apparent decreased thickness of epithelial layer which was in agreement with ^[24] who stated that upon corneal examination of SOF treated group showed some areas with apparent decrease in thickness of the epithelium.

In the present study, upon short-term (Subgroup IIA) and long-term (Subgroup IIB) of SOF administration, the histological results showed the epithelial cells with lightly stained cytoplasm and pale stained nuclei. Based on a study done by ^[25] the effect of SOF on cerebral cortex was recorded as a distortion in the shape of the neurons and reduction of the nuclei which were surrounded by vacuolated pale regions most probably apoptotic cells.

Vacuolated cells with clear cytoplasm were detected in basal and para basal cells of the epithelium of the subgroups IIA & IIB in the current study, these vacuolated cells increased with the increase of the duration in Subgroup IIB. This finding matched the conclusion made by ^[23], that the mechanism of SOF-induced renal tubular necrosis was thought to be concentration-duration dependent. Our results also are in agreement with ^[26] who suggested that SOF has a cytotoxic effect in lower concentrations but on the other hand, SOF has antioxidant effect in opposite directions at higher concentrations so they concluded that SOF despite being toxic and pro-oxidant at lower concentrations, it acts as protective and antioxidant at higher concentrations.

The findings of ^[27, 28] explained the relation between vacuolar degeneration and destruction or injury of mitochondria, because physiologically,

mitochondria are involved in the maintenance of Ca^{2+} homeostasis mainly. When the cellular metabolism gets disturbed, allowing sodium ions to enter the cell, it may be interpreted as vacuolar degeneration. Large macromolecules within the injured cell were broken down by the osmotic impact, resulting in the formation of cytoplasmic vacuoles. However, Ca^{2+} overload in mitochondria leads to organelle damage. So irreversible damage of mitochondria caused by Ca^{2+} excess often appears as severe swelling of the organelles.

Rat submandibular salivary gland was an example, ^[29] documented that most parenchymal elements were distorted with vacuolated apoptotic cells and ghost-like structures after treatment with SOF for 5 weeks.

In the current study in Subgroup IIB some cell of the prickle cell layer appeared swollen and some cells appeared to have diffuse cytoplasmic vacuolization as well. Staining affinity is often diminished when cells are swollen or has vacuolization, giving the cells the pale appearance. Vacuolar degeneration or ballooning degeneration are terms used to describe this sort of alteration^[30]. Cell swelling is not lethal per se, as ^[31] pointed out, it can signify relatively a mild injury; nonetheless, cells that are seriously injured usually undergo a phase of swelling as well. Therefore, it's important to note that lethally injured cells that were repaired in the early stages of death might be misinterpreted as slightly injured, when actually they are greatly damaged. In addition, cellular edema was reported to develop whenever an increased volume of fluid accumulates in the tissues, limiting the diffusional clearance of harmful byproducts of cellular metabolism^[32].

According to ^[33], these alterations in the buccal mucosa were deemed as a sign of toxicity, they ascribed these changes to cell death due to mitochondrial toxicity and an overabundance of reactive oxygen species (ROS). Mitochondria have a crucial role in the generation of ROS,

which are physiologically formed during oxidative phosphorylation. When there is a variance between the production of ROS and the cellular antioxidant defenses oxidative stress occurs. Protein synthesis and metabolism were disrupted, organelles degraded, and cells died via apoptosis as a result of oxidative stress. Therefore, it was concluded that increased ROS production could cause obvious degenerative changes in mitochondria [29, 34]. This is concomitant with a study by [35] observing the effect of SOF on alveolar process as it showed mitochondrial swelling and dysfunction that could lead to increased ROS production.

According to [19, 36] who correlated their findings of the degeneration of the salivary glands during the administration of Sovaldi™ to the increase of ROS production, the mechanism of Sovaldi™ degenerative effect that was detected in this study could be thus relied on ROS accumulation.

Loss of basilar polarity observed in Subgroup IIA could be linked to the increased production of ROS as suggested by [37], they demonstrated that loss of polarity in mammary acini was linked to increased ROS production, whereas increased ROS production is sufficient to disrupt basal polarity.

The finding of basilar hyperplasia in Subgroup IIA in this study is in agreement with [38] that proved that SOF upregulates several genes that were associated with increased cell proliferation and migration.

In the current study, morphologically disturbed multiple epithelial rete pegs with irregular thickness were seen in Subgroup IIA but; in Subgroup IIB the basement membrane was less scalloped, which indicates a decline in the surface area at the interface between the epithelium and the connective tissue causing less communication and nutrient transfer between the epithelium and the connective tissue. Generally, the morphogenesis of rete pegs is a result of the oral epithelium, which has active proliferated keratinocytes, invading the lamina propria, and in

this process, the migration of keratinocytes during the morphogenesis of rete peg somewhat is similar to the invasion of malignant epithelial cells in the carcinomas, with the difference being that the former is under control while the latter is not [39].

In this study both subgroup IIA and subgroup IIB showed the underlying lamina propria is disarranged with multiple spaces, our result also revealed wide separation of the connective tissue collagen fibers, so SOF might be the one causing disarrangement to the collagen bundles as explained by [29] who revealed the decrease in the submandibular salivary gland fibrous connective tissue thickness after SOF administration. As well as [24] found wide separations and disarrangements of the collagen fibers bundles in addition to upregulation of fibronectin expression in the retina of SOF treated rats. [40] Concluded that SOF had an anti-fibrotic outcome leading to decreased collagen fibers arrangement.

In the current study, the submucosa appeared with areas of separations especially surrounding the muscle layer in subgroup IIA. Obvious degenerative changes were seen mainly in Subgroup IIB. This finding is in agreement with [41] where they found that Sovaldi administration caused muscle fiber clumping, hyaline degeneration, fatty infiltration and fibrosis of both intrinsic tongue and masseter muscles with variable degrees of degenerative signs.

Regarding the dilatation of the vascular supply, the enlargement of blood vessels was monitored in both subgroup IIA & IIB of the experimental group and it could be a side effect of Sovaldi™, these findings were in agreement with [25] who found vascular dilatation and extravasation of cerebral cortex blood vessels following 5 weeks of SOF administration. According to [42] unbearable inflammation may lead to a microcirculatory disruption causing complete loss of capillary integrity. According to these accumulating data by [43, 44] they indicate that ROS are signaling molecules which can influence multiple acute

vascular activities including vasodilatation, vasoconstriction and vascular permeability, and long-term vascular alterations such as structural remodeling of vessel parts and vascular beds.

Proliferating cell nuclear antigen (PCNA) and Ki-67 antigen are the two most common immunohistochemical markers frequently used to study cell proliferation. Ki-67 has been recorded to be an excellent marker for estimating the growth fraction in both normal and malignant human tissue, and it is currently utilized as the golden standard for assessing cell proliferation instead of PCNA since it is less impacted by internal and external factors. Antigen Ki-67 also commonly known as Ki-67 or MKI67 (Marker of proliferation Ki-67), is a protein in humans that is encoded by the MKI67 gene [45, 46, 47]. Its function as a biological marker of mitotic activity is aided by its nuclear expression throughout a specific period of the cell cycle. It also has a substantially shorter half-life, resulting in producing less staining after cells have gone through proliferative stage. Its presence therefore suggests that it is in the proliferative stage rather than being only residual evidence of the cell that has passed through the stage. The fraction of Ki-67 positive cells is frequently associated to the disease's prognosis. Ki-67 marker has been extensively studied in oral epithelial dysplasia [48, 49].

In our study, the Ki-67 expression was detected in all specimens of the control group, Subgroup IA & IB, where normal oral epithelium with its parabasal layer showed intense staining which is in accordance with a previous report by [47] who had the same results in normal tissue staining.

According to this research, the immunohistochemical marker Ki-67, showed statistical significant decrease in area percentage of positively stained Ki-67 cells in both subgroups IIA & IIB, when compared to the control group. The area percentage was also significantly decreased in Subgroup IIB when compared to subgroup IIA. In this study, the presence of Ki67 in the deep layers of the

epithelium suggests that despite cell loss from the surface by desquamation, cell division and apoptosis seemed to be disturbed. Other investigators have reached the same results and found that SOF was disturbing the regulation of cell proliferation, which may lead to apoptosis [38, 50, 51] who suggested that the use of DAADs can affect cellular proliferation especially on grafted tissues.

This is also in agreement with these studies that suggests SOF cause overproduction of (ROS) which leads to disorder of metabolism, degeneration of organelles and cell death by apoptosis [23, 29, 35, 41].

CONCLUSIONS

From our study, we concluded that short and long term SOF administration resulted in degenerative signs in buccal mucosa of albino rats with a decrease in area percentage of Ki-67 immunopositivity which was time dependent. Further studies are recommended to investigate the effect of SOF on different oral tissues.

REFERENCES

1. Lawitz E., Mangia A., Wyles D., Rodriguez-Torres M., Hassanein T., Gordon S. C., Schultz M., Davis M. N., Kayali Z., Reddy K. R., Jacobson I. M., Kowdley K. V., Nyberg L., Subramanian G. M., Hyland R. H., Arterburn S., Jiang D., McNally J., Brainard D., Symonds W. T., and Gane E. J. (2013): Sofosbuvir for previously untreated chronic hepatitis C infection. *The New England journal of medicine*; 368(20): 1878–1887.
2. McQuaid T., Savini C., and Seyedkazemi S., (2015): Sofosbuvir, a Significant Paradigm Change in HCV Treatment. *Journal of Clinical and Translational Hepatology*; 3: 27-35.
3. Kowdley Kv., Lawitz E., and Poordad F., (2014): Phase 2b trial of interferon free therapy for hepatitis C virus genotype1. *N Engl J Med*; 370: 222-232.
4. Zoulim, F., Liang, T. J., Gerbes, A. L., Aghemo, A., Deuffic-Burban, S., Dusheiko, G., Fried, M. W., Pol, S., Rockstroh, J. K., Terrault, N. A., & Wiktor, S. (2015): Hepatitis C virus treatment in the real world: optimising treatment and access to therapies. *Gut*; 64(11): 1824–1833.

5. Noell B.C., Besur S.V., and deLemos A.S. (2015): Changing the face of hepatitis C management - the design and development of sofosbuvir. *Drug design, development and therapy*; 9: 2367–2374.
6. Zeng Q.L., Zhang J.Y., Zhang Z., Wang L.F., and Wang F.S. (2013): Sofosbuvir and ABT-450: terminator of hepatitis C virus. *World journal of gastroenterology*; 19(21): 3199–3206.
7. Bhatia H., Singh H., and Grewal N. (2014): Sofosbuvir: A novel treatment option for chronic hepatitis C infection. *J PharmacolPharmacother*; 4: 278-284.
8. Kayali, Z., and Schmidt, W. N. (2014): Finally sofosbuvir: an oral anti-HCV drug with wide performance capability. *Pharmacogenomics and personalized medicine*; 7: 387–398.
9. Shin J., Seol I., and Son C. (2010): Interpretation of Animal Dose and Human Equivalent Dose for Drug Development. *The Journal of Korean Oriental Medicine*; 31(3): 1–7.
10. Bancroft J., Suvarna K., and Layton C. (2018): *Bancroft's Theory and Practice of Histological Techniques* 8th edition. Elsevier: 77-103.
11. Gerdes J., Schwab U., Lemke H., and Stein H. (1983): Production of a mouse monoclonal antibody reactive with a human nuclear antigen associated with cell proliferation. *Int. J. Cancer*; 31(1): 13–20.
12. Kinra P., and Malik A. (2020): Ki 67: Are we counting it right? *Indian journal of pathology & microbiology*; 63(1): 98–99.
13. Specht K., Richter T., Müller U., Walch A., Werner M., & Höfler H. (2001): Quantitative gene expression analysis in micro-dissected archival formalin-fixed and paraffin-embedded tumor tissue. *The American journal of pathology*; 158(2): 419-429.
14. Oladele A., Hassan Y., Victor O.E., Toluwalope W.H., Adegoke A. (2021): Prognostic Value of Amac and Ki-67 in Progression of Prostate Cancer. *Quest Journals Journal of Medical and Dental*; 8(2): 41-51.
15. McCaughan G., McHutchison J., and Pawlotsky J., (2011): *Advanced Therapy for Hepatitis C*. UK: WILEY BLACKWELL; 1st edition: 98-101.
16. Sulkowski M.S., Vargas H.E., Di Bisceglie A.M., Kuo A., Reddy K.R., Lim J.K., Morelli G., Darling J.M., Feld J.J., Brown R.S., Frazier L.M., Stewart T.G., Fried M.W., Nelson D.R., Jacobson I.M., and HCV-TARGET Study Group (2016): Effectiveness of Simeprevir Plus Sofosbuvir, With or Without Ribavirin, in Real-World Patients with HCV Genotype 1 Infection. *Gastroenterology*; 150(2): 419–429.
17. Elgharably A., Gomaa I., Crossey M., Norsworthy J., Waked I., and Taylor-Robinson D. (2017): Hepatitis C in Egypt – past, present, and future. *International Journal of General Medicine*; 10(1): 1–6.
18. Sengupta P. (2013): The laboratory rat: relating its age with humans. *International journal of preventive medicine*; 4(6): 624-30.
19. Salem Z. A., Elbaz D. A., and Farag D. B. E. (2017): Effect of an Anti-Hepatitis C Viral Drug on Rat Submandibular Salivary Gland. *Egyptian Dental Journal*; 63(1): 1-9.
20. Seelagan D., and Noujaim S.E. (2007): A pictorial review of the anatomy and common pathology of the buccal space, the overlooked space. *Applied Radiology*; 36(1): 20-28.
21. Squier C. and Brogden K. (2010): *Human Oral Mucosa: Development, Structure and Function*. John Wiley & Sons; 1st Edition: 20-41.
22. Leifert W.R., François M., Thomas P., Luther E., Holden E., Fenech M., (2011): Chapter 13 Automation of the Buccal Micronucleus Cytome Assay Using Laser Scanning Cytometry ,*Methods in Cell Biology*, Academic Press; (102): 321-339.
23. El Gharabawy G., Abdallah E., Kaabo H., and Abdel Aleem A. (2019): Histological Effects of Sofosbuvir on the Kidney of Male Albino Rats and the Possible Protective Role of Vitamin C. *The Egyptian Journal of Hospital Medicine*; 76(1):3335-3354.
24. Issa N. M., and El-Sherif N. M. (2017): Histological and Immunohistochemical Studies on the Cornea and Retina of Sofosbuvir Treated Rats. *Austin J Anat*; 4(2): 1068.
25. Issa N. M., and El-Sherif N. M. (2017): Light and electronic histological studies to the effect of Sofosbuvir on the visual cerebral cortex of adult male albino rat. *Journal of American Science*; 13(4): 79-87.
26. Yousefsani B.S., Nabavi N., and Pourahmad J. (2020): Contrasting Role of Dose Increase in Modulating Sofosbuvir-Induced Hepatocyte Toxicity. *Drug research*; 70(4): 137–144.
27. Dong Z., Saikumar P., Weinberg J., and Venkatachalam M. (2006): Calcium in cell injury and death. *Annual review of pathology*; 1: 405-34.
28. Shubin A.V., Demidyuk I.V., Komissarov A.A., Rafieva L.M., and Kostrov S.V. (2016): Cytoplasmic vacuolization in cell death and survival. *Oncotarget*, 7(34): 55863–55889.
29. Abdeen A., Essawy T., and Mohammed S. (2019): Effect

- of Sofosbuvir Administration and Its Withdrawal on the Submandibular Salivary Gland of Adult Male Albino Rats: A Histological and Ultra-Structural Study. *Maced J Med Sci*; 7(23):4101-4109.
30. Wanda M. H. and Wallig M. (2010): *Fundamentals of Toxicologic Pathology*. ACADEMIC PRESS; 2nd Edition: 78-90.
 31. Lemasters J.J. (2010): *Comprehensive Toxicology (Second Edition)*, Cyto-lethality 1.12. Editor(s): Charlene A. McQueen, Elsevier; 245-268.
 32. Scallan J., Huxley V. H., and Korthuis R. J. (2010): *Capillary Fluid Exchange: Regulation, Functions, and Pathology*. Morgan & Claypool Life Sciences; 2nd edition: 97-109.
 33. Balaban R., Nemoto S., and Finkel T. (2005): Mitochondria, oxidants, and aging. *Cell*; 120(4):483-495.
 34. Merli A., Capaldi R. A., Ackrell B. A. C., and Kearney E. B. (1979): Arrangement of complex II (succinate-ubiquinone reductase) in the mitochondrial inner membrane. *Biochemistry*; 18(8): 1393-1400.
 35. Farag D., El-Baz D.A., and Salem Z.A. (2018): Alveolar process changes associated with administration of nucleos(t)ide analogue (sofosbuvir) in rat model. *Dental and medical problems*; 55(1): 11-16.
 36. Saad A. F., Aboushady I.M., and Mehanni S. (2019): Extra Hepatic Effects of Sofosbuvir on a Serous Model of Major and Minor Salivary Glands in Albino Rats: *The Egyptian Journal of Histology*; 43: 325-339.
 37. Li L., Chen J., Xiong G., St Clair D. K., Xu W., and Xu R. (2017): Increased ROS production in non-polarized mammary epithelial cells induces monocyte infiltration in 3D culture. *Journal of cell science*; 130(1): 190-202.
 38. Tsai W., Cheng J., Liu P., Chang T., Chang Y., Sun W., Chen W., and Shu C. (2020): Sofosbuvir-Upregulated Genes Facilitate The Development of Hepatocellular Carcinoma. *Research Square*; 10.21203(1): 130882.
 39. Xiong X., Wu T., and He S. (2013): Physical forces make rete ridges in oral mucosa. *Medical hypotheses*; 81(5): 883-886.
 40. El Sisi A., and Zakaria S. (2019): Potential Anti-Fibrotic Effect of Direct Acting Antiviral Drugs on CCl4 Induced Hepatic Fibrosis in Rats. *Egyptian Journal of Basic and Clinical Pharmacology*; 9:101414.
 41. Mehanny S.S., Salem Z.A., and Maria M.K.M., (2019): The Histopathological Effects of Sovaldi on Masseter Muscles in Albino Rats (an animal study). *Egyptian Dental Journal*; 65: 1395:1403.
 42. Mubarak R. (2012): Effect of red bull energy drink on rats' submandibular salivary glands (light and electron microscopic study). *The Journal of American Science*; 8: 366-372.
 43. Tretter L., Patocs A., and Chinopoulos C. (2016): Succinate, an intermediate in metabolism, signal transduction, ROS, hypoxia, and tumorigenesis. *Biochimica et Biophysica Acta – Bioenergetics*; 1857(8): 1086-1101.
 44. Li H., Horke S., and Forstermann U., (2014): Vascular oxidative stress, nitric oxide and atherosclerosis. *Atherosclerosis*; 237: 208-219.
 45. Bullwinkel J., Baron-Lühr B., Lüdemann A., Wohlenberg C., Gerdes J., and Scholzen T. (2006): Ki-67 protein is associated with ribosomal RNA transcription in quiescent and proliferating cells. *J. Cell Physiology*; 206 (3):624-35.
 46. Ntzeros K., Stanier P., Mazis D., Kritikos N., Rozis M., Anesidis E., Antoniou C., and Stamatakos M. (2015): MKI67 (marker of proliferation Ki-67). *Atlas of Genetics and Cytogenetics in Oncology and Haematology*; 19(2): 105-116.
 47. Hegazy E., Elmansy M., and Mahmoud E. (2018): Immunohistochemical Evaluation of Bcl-2 and Ki-67 in Buccal Mucosa of Induced- Immunosuppressed Albino Rats. *Egyptian Dental Journal*; 64(3): 2297-2304.
 48. Bologna-Molina R., Mosqueda-Taylor A., Molina-Frechero N., Mori-Estevez A. D., and Sánchez-Acuña G. (2013): Comparison of the value of PCNA and Ki-67 as markers of cell proliferation in ameloblastic tumors. *Medicina oral, patologia oral y cirugía bucal*; 18(2): 174-179.
 49. Shi P., Zhong J., Hong J., Huang R., Wang K., and Chen Y. (2016): Automated Ki-67 Quantification of Immunohistochemical Staining Image of Human Nasopharyngeal Carcinoma Xenografts. *Scientific Reports*; 6: 1-9.
 50. Dyson J.K., Hutchinson J., Harrison L., Rotimi O., Tiniakos D., Foster G.R., Aldersley M A., and McPherson S. (2016): Liver toxicity associated with sofosbuvir, an NS5A inhibitor and ribavirin use. *Journal of hepatology*, 64(1), 234-238.
 51. Teegen E. M., Dürr M., Maurer M. M., Eurich F., Vollbort A., Globke B., Bahra M., Blaeker H., Pratschke J., and Eurich D. (2019): Evaluation of histological dynamics, kidney function and diabetes in liver transplant patients after antiviral treatment with direct-acting antivirals: Therapy of HCV-recurrence. *Transplant infectious disease*; 370: 211-221.